Available online at www.sciencedirect.com

ScienceDirect

Nuclear and Particle Physics Proceedings 273–275 (2016) 452–458

www.elsevier.com/locate/nppp

A first walk on the DarkSide

S. Davini[a,*], P. Agnes[b], T. Alexander[c], A. Alton[d], K. Arisaka[e], H. O. Back[f], B. Baldin[g], K. Biery[g], G. Bonfini[h], M. Bossa[i], A. Brigatti[j], J. Brodsky[f], F. Budano[k], F. Calaprice[f], N. Canci[e], A. Candela[h], M. Cariello[l], P. Cavalcante[h], A. Chavarria[m], A. Chepurnov[n], A. G. Cocco[o], D. D'Angelo[j], M. D'Incecco[h], M. De Deo[h], A. Derbin[p], A. Devoto[q], F. Di Eusanio[f], E. Edkins[r], A. Empl[a], A. Fan[e], G. Fiorillo[o], K. Fomenko[s], D. Franco[b], F. Gabriele[h], C. Galbiati[f], A. Goretti[f], L. Grandi[m], M. Y. Guan[t], Y. Guardincerri[g], B. Hackett[r], K. Herner[g], E. V. Hungerford[a], Al. Ianni[h], An. Ianni[f], C. Kendziora[g], G. Koh[f], D. Korablev[s], G. Korga[a], A. Kurlej[c], P. X. Li[t], P. Lombardi[j], S. Luitz[u], I. Machulin[v], A. Mandarano[j], S. Mari[k], J. Maricic[r], L. Marini[k], C. J. Martoff[w], P. D. Meyers[f], D. Montanari[g], M. Montuschi[h], M. E. Monzani[u], P. Musico[l], S. Odrowski[h], M. Orsini[h], F. Ortica[x], L. Pagani[l], E. Pantic[e], L. Papp[y], S. Parmeggiano[j], N. Pelliccia[x], S. Perasso[b], A. Pocar[c], S. Pordes[g], H. Qian[f], K. Randle[c], G. Ranucci[j], A. Razeto[h], B. Reinhold[r], A. Renshaw[e], A. Romani[x], B. Rossi[f], N. Rossi[h], S. D. Rountree[y], D. Sablone[a], R. Saldanha[m], W. Sands[f], E. Segreto[h], E. Shields[f], O. Smirnov[s], A. Sotnikov[s], C. Stanford[f], Y. Suvorov[e], J. Tatarowicz[w], G. Testera[l], A. Tonazzo[b], E. Unzhakov[p], R.B. Vogelaar[y], M. Wada[f], S. Walker[o], H. Wang[e], A. Watson[w], S. Westerdale[f], M. Wojcik[z], X. Xiang[f], J. Xu[f], C. G. Yang[t], J. Yoo[g], S. Zavatarelli[l], A. Zec[c], C. Zhu[f], G. Zuzel[z]

[a] *Department of Physics, University of Houston, Houston, TX 77204, USA*
[b] *APC, Université Paris Diderot, Sorbonne Paris Cité, Paris 75205, France*
[c] *Physics Department, University of Massachusetts, Amherst, MA 01003, USA*
[d] *Physics and Astronomy Department, Augustana College, Sioux Falls, SD 57197, USA*
[e] *Physics and Astronomy Department, University of California, Los Angeles, CA 90095, USA*
[f] *Physics Department, Princeton University, Princeton, NJ 08544, USA*
[g] *Fermi National Accelerator Laboratory, Batavia, IL 60510, USA*
[h] *Laboratori Nazionali del Gran Sasso, Assergi (AQ) 67010, Italy*
[i] *Gran Sasso Science Institute, L'Aquila 67100, Italy*
[j] *Physics Department, Università degli Studi and INFN, Milano 20133, Italy*
[k] *Physics Department, Università degli Studi Roma Tre and INFN, Roma 00146, Italy*
[l] *Physics Department, Università degli Studi and INFN, Genova 16146, Italy*
[m] *Kavli Institute, Enrico Fermi Institute and Dept. of Physics, University of Chicago, Chicago, IL 60637, USA*
[n] *Skobeltsyn Institute of Nuclear Physics, Lomonosov Moscow State University, Moscow 119991, Russia*
[o] *Physics Department, Università degli Studi Federico II and INFN, Napoli 80126, Italy*
[p] *Saint Petersburg Nuclear Physics Institute, Gatchina 188350, Russia*
[q] *Physics Department, Università degli Studi and INFN, Cagliari 09042, Italy*
[r] *Department of Physics and Astronomy, University of Hawai'i, Honolulu, HI 96822, USA*
[s] *Joint Institute for Nuclear Research, Dubna 141980, Russia*
[t] *Institute of High Energy Physics, Beijing 100049, China*
[u] *SLAC National Accelerator Laboratory, Menlo Park, CA 94025, USA*
[v] *National Research Nuclear University Moscow Engineering Physics Institute, 115409 Moscow, Russia*
[w] *Physics Department, Temple University, Philadelphia, PA 19122, USA*
[x] *Chemistry, Biology and Biotechnology Department, Università degli Studi and INFN, Perugia 06123, Italy*
[y] *Physics Department, Virginia Tech, Blacksburg, VA 24061, USA*
[z] *Smoluchowski Institute of Physics, Jagiellonian University, Krakow 30059, Poland*

Abstract

DarkSide-50 (DS-50) at Gran Sasso underground laboratory (LNGS), Italy, is a direct dark matter search experiment based on a TPC with liquid argon. DS-50 has completed its first dark matter run using atmospheric argon as target. The DS-50 detector performances and the results of the first physics run are reviewed in this proceeding.

Keywords: Dark matter, Scintillation detectors

http://dx.doi.org/10.1016/j.nuclphysbps.2015.09.066

1. Introduction

Many experimental results in cosmology and astrophysics brings pieces of evidence for the existence of Dark Matter. Such results include measurements of the galactic rotation curves, galaxy clusters, gravitational lensing, and the multipole power spectrum of the cosmic microwave background radiation. The most natural explanation for such measurements is the presence of a large amount of invisible non-baryonic matter, with a total energy density roughly five times that of baryonic matter. Dark Matter must interact very weakly with electromagnetic radiation (non-emitting and non-absorbing photons) and must be stable on cosmological time scales (otherwise it would have decayed by now).

One of the favored candidates of Dark Matter are Weakly Interactive Massive Particles (WIMPs), neutral particles with mass ∼100 GeV and cross-section $\sim 10^{-47}\,\mathrm{cm}^2$, that can be gravitationally trapped inside our galaxy [1]. If WIMPs exist, they should occasionally interact with an atomic nucleus, causing the nucleus to recoil with an amount of kinetic energy of the order of few tens of keV.

Direct observation of WIMP-nuclei collisions in a laboratory detector plays a key role in dark matter searches. However, it poses at the same time significant experimental challenges, as the expected signals are low in energy (below 100 keV) and very rare (a few interactions per year per ton of target, based on existing limits). Ultra low background and underground detectors with target masses of 0.1-10 tons are mandatory to detect these WIMPs.

The DarkSide project attempts to detect WIMP-induced nuclear recoils using two-phase Argon time projection chambers (TPCs) with scalable, zero-background technology. Argon TPCs, which are described in detail in [2], measure, by optical means, both the energy deposited and the ionization charge produced by particle interactions in their liquid active volumes.

The largest challenge in searching for dark matter is the suppression of the rate of background events to below the very low WIMP interaction rates (a few events per ton-year) to which current dark matter experiments are sensitive. One reason that makes Argon a promising medium for dark matter searches is that it provides the ability, using pulse shape discrimination (PSD) based on the time profile of the primary scintillation signal, to reject electron recoil background events to levels in excess of 10^{-8} [2, 3]. In two-phase operation, additional discrimination can be achieved using the ratio of scintillation to ionization for each event [2].

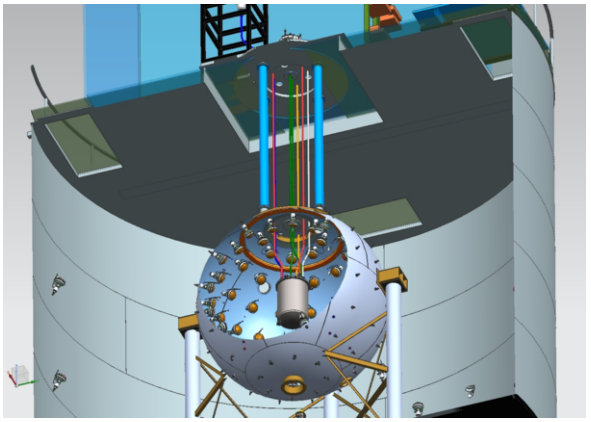

Figure 1: The nested detector system of DarkSide-50 (DS-50). The outermost dark gray cylinder is the Water Cherenkov Detector (WCD), the sphere is the Liquid Scintillator Veto (LSV), and the gray cylinder at the centre of the sphere is the Liquid Argon TPC (LAr TPC).

One of the goal of DarkSide-50 is to conduct a dark matter search with its TPC filled with underground Argon naturally depleted in radioactive ^{39}Ar. The final purification of the underground Argon supply is still in progress. A dark matter search with a present exposure of (1423 ± 67) kg, using a fill of atmospheric argon, has been conducted meanwhile [4].

A key feature of DarkSide is its water and liquid scintillator veto system with further suppresses radiogenic and cosmogenic backgrounds. During this period, the liquid scintillator veto performance was limited due to an unexpectedly high content of ^{14}C int the trimethyl borate (TMB) that was added as a neutron capture agent. The veto performance nevertheless appears to have been adequate to measure and suppress the very low rate of neutron-induced events in this present data sample. The TMB has been removed since June 2014 and a source of low-activity TMB identified.

2. The DarkSide-50 detector

The DarkSide-50 apparatus consists of three nested detectors, see Fig. 1. From the centre outward, the three detectors are: the Liquid Argon Time Projection Chamber (LAr TPC), which is the dark matter detector; the organic Liquid Scintillator Veto (LSV), serving as shielding and as anti-coincidence for radiogenic and cosmogenic neutrons, γ -rays and cosmic muons; and the Water Cherenkov Detector (WCD), serving as shielding

*Corresponding author
Email address: stefano.davini@gmail.com (S. Davini)

and as anti-coincidence for cosmic muons [5, 6, 7, 8]. The detector system is located in Hall C of LNGS at a depth of 3800 meter-water-equivalent, in close proximity to and sharing many facilities with, the Borexino solar neutrino detector [9, 10].

The LAr TPC can exploit pulse shape discrimination and the ratio of scintillation to ionization to reject beta and gamma background in favor of the nuclear recoil events expected from WIMP scattering [2, 3]. It can also exploit the TPC's spatial resolution to reject surface backgrounds and to reject multi-sited events. Events due to neutrons from cosmogenic sources and from radioactive contamination in the detector components, which also produce nuclear recoils, are suppressed by the combined action of the neutron and cosmic ray vetoes. The liquid scintillator also provides additional rejection of γ-ray background from the detector materials. The water-plus-liquid scintillator design was motivated in part by the success of this shielding concept in achieving very low backgrounds in Borexino [9, 11, 12].

The WCD is an 11 m-diameter, 10 m-high cylindrical tank filled with high purity water. The tank was originally part of the Borexino Counting Test Facility. The inside surface of the tank is covered with a laminated Tyvek-polyethylene-Tyvek reflector. An array of 80 ETL 9351 8" PMTs, with 27% average quantum efficiency at 420 nm, is mounted on the side and bottom of the water tank to detect Cherenkov photons produced by muons or other relativistic particles traversing the water.

The LSV is a 4 m-diameter stainless steel sphere filled with 30 tons of borated liquid scintillator. The scintillator consists of equal amounts of pseudocumene (PC) and trimethyl borate (TMB), with the wavelength shifter Diphenyloxazole (PPO) at a concentration of 3 g/L. The sphere is lined with Lumirror reflecting foils. An array of 110 Hamamatsu R5912 8" PMTs, with low-radioactivity glass bulbs and high-quantum-efficiency photocathodes (37% average quantum efficiency at 408 nm) is mounted on the inside surface of the sphere to detect scintillation photons.

The neutron-capture reaction ^{10}B(n, α)^{7}Li makes the borated scintillator a very effective veto of neutron background [13]. The TMB, B(OCH$_3$)$_3$, contains natural Boron which has a 20 % natural abundance of ^{10}B with its very large (3840 barn) thermal neutron capture cross section. The thermal neutron capture time in the borated scintillator is calculated to be just 2.2 μs, compared to 250 μs for pure PC [9].

The ^{10}B neutron capture proceeds to the ^{7}Li ground state with branching ratio 6.4%, producing a 1775 keV α particle, and to a ^{7}Li excited state with branching ratio 93.6%, producing a 1471 keV α particle and a gamma-ray of 478 keV. Because of quenching, the scintillation light output of the capture to ^{7}Li (g.s.) is expected to be in the electron-equivalent range 40−50 keV. The measured LSV photoelectron (PE) yield is (0.53 ± 0.02) PE/keV, making this quenched energy detectable. The high ^{14}C decay rate in the LSV and the fact that its spectrum covers the signal expected from the α's from neutron capture on ^{10}B, affected the effectiveness of the neutron veto in the present data set [13].

The DS-50 LAr TPC, as shown in Fig. 1, is contained in a stainless steel cryostat that is supported at the centre of the LSV. The design of the DS-50 LAr TPC was based on that of the DarkSide-10 prototype [14].

Ionizing events in the active volume of the LAr TPC result in a prompt scintillation signal called "S1". Ionization electrons escaping recombination are drifted by the TPC electric field to the surface of the liquid argon, where a stronger electric field extracts them into an argon gas layer between the LAr surface and the TPC anode. The electric field in the gas is large enough to accelerate the electrons so that they excite the argon, resulting in a secondary scintillation signal, "S2", proportional to the collected ionization. Both the scintillation signal S1 and the ionization signal S2 are measured by the same PMT array. The temporal pulse shape of the S1 signal provides discrimination between nuclear-recoil and electron-recoil events. The S2 signal allows the three-dimensional position of the energy deposition to be determined and, in combination with S1, provides further discrimination of signal from background.

In liquid argon, scintillation is initiated by excitation and recombination after ionization. The 128 nm scintillation photons are emitted from two nearly degenerate excimer states, a long-lived (1.6 μs) triplet state, and a short-lived (6 ns) singlet state. The difference in ionization density between nuclear recoils (from WIMP or neutron scattering) and electron recoils, (from β and γ radiation) produces a significant difference in the radiative decay ratio of these states and hence in the time profile of the S1 scintillation light. Nuclear recoils have more of the fast scintillation component than electron recoils, providing a very powerful "pulse shape discrimination" (PSD) between electron backgrounds and nuclear-recoil signals [3].

In the analysis presented in [4], we use a simple PSD parameter, f_{90}, defined as the fraction of the S1 signal that occurs in the first 90 ns of the pulse, which is typically $\sim$ 0.3 for electron recoils and $\sim$ 0.7 for nuclear recoils. For electron recoil events, the low density of electron-ion pairs also results in less recombination and therefore more free electrons, compared to a nuclear recoil track of the same energy deposition. The ra-

tio of ionization (measured by S2) to scintillation (S1) can therefore also be used to distinguish electron recoils from nuclear recoils. In this paper, we use PSD and basic cuts on S2 to reduce backgrounds, but we do not yet exploit the discrimination power of S2/S1, which is still being developed.

Additional information on the detectors employed in the DarkSide project can be found in [4, 14, 15, 16, 17].

3. Data acquisition and event reconstruction

The data acquisition system of DS-50 consists of two main sub-systems, handling the TPC and the vetoes respectively. The ground-referenced anodic signal from each of the thirty-eight TPC photomultiplier tube is first amplified by a cryogenic head-amplifier located in liquid argon on the phototube base divider. This first stage allows us to operate the PMTs at lower gain (typically 4×10^5), reducing the occurrence of flashers. The AC-coupled cold amplifiers are configured to provide a gain of a factor 3 with 150 MHz bandwidth, 2.4 ns symmetric rise/fall times, a 5.8 ns low-frequency time constant and a maximum peak output of 3 V into a 50 Ω terminated signal cable. The signal undergoes then a second stage that duplicates it into multiple branches. One copy undergoes a ×10 amplification and is used to form the trigger, feeding high speed discriminators with adjustable threshold. Another ×10 amplified copy, is filtered and multiplexed and then sent directly to a set of 12 bit, 250 MSamples/second, digitizers (CAEN 1720).

In a similar way, the anodic signals from LSV and WCD phototubes undergo amplification and duplication by means of a custom front-end board. A ×10 amplified signal for each PMT is digitised with NI PXIe-5162 National Instruments modules, by sampling them at 1.25 GSamples/second with 10 bit resolution. Zero-suppression is performed on the fly and only sections of the waveform around identified peaks above threshold are are stored. The zero-suppression threshold was set to 1/3 of a photoelectron for routine data taking.

The DAQ sub-systems are handled by a common run controller that can be configured to permit different acquisition modes, sharing a global trigger among all three detectors or allowing independent triggers. In the first configuration the photomultiplier signals from the TPC and vetoes are acquired when at least three TPC PMTs detect within a 100 ns window more than 0.6 PE each. This implementation has been used to acquire background runs for studying PSD, where information from the veto are needed to tag and reject specific classes of TPC events (i.e. background induced by γ-rays or neutrons). Veto acquisition windows as long as 70 μs are selected in order to search for possible delayed neutron-captures: while neutron capture times of the order of few μs are expected in boron-loaded liquid scintillator, our Monte Carlo simulation shows that some neutron induced events release their energy can be detected by the LSV even few tens of μs after the interaction in the TPC, due to capture occurring in the material surrounding the TPC, characterised by much longer capture times.

PMT gain calibrations or energy scale calibrations, since related to a single detector, have been normally performed with the independent trigger configuration. The calibration of the photomultiplier-tube gains and the study of their charge response are performed for the three detectors by injecting light from pulsed laser diodes into their sensitive volumes by means of dedicated optical fibres.

An offline reconstruction code is used to analyze the stored waveforms from the TPC and the vetoes photomultiplier tubes. As far as the TPC is concerned, signals from each channel scaled by the corresponding single photoelectron mean are added to form a sum waveform that is used for identifying the pulses in the trigger gate and their start time. Since coherent noise among channels is present, once identified the time window of interest for each pulse, we estimate the main parameters on each channel, that exhibits a signal/noise ratio more favourable with respect to the sum. A moving-average baseline algorithm is used to estimate the baseline on each channel. In the regions where the signal overcomes a baseline-related threshold the baseline is estimated by performing a linear interpolation between the sample before and after the identified region. This permits to follow slow baseline variations (at the μs scale) and accurately evaluate the integrals of the baseline subtracted signals for each pulse.

Due to the use of DAQ-level zero-suppression, reconstruction of LSV and WCD signals is different from the TPC reconstruction. Pulses are naturally defined as the non-zero portion of each raw waveform for each channel. The DAQ records 20 ns before and after the waveform rises above and drops below, respectively, the zero-suppression threshold. For each pulse, the first 15 samples are averaged to define a baseline, which is subtracted from the waveform. Each channel is then scaled by the corresponding single photoelectron mean and the channels in each veto detector are summed together. A clustering algorithm on the sum waveform identifies physical events in the LSV and WCD. To handle the high pile-up rate in the LSV due to ^{14}C, the algorithm is a "top-down" iterative process of searching for clusters from largest to smallest. These clusters are used only for building the ^{14}C spectrum and determin-

ing the light yield of the LSV. Identification of coincident signals between LSV and TPC uses fixed regions of interest of the sum waveform and is described later. For tagging of muons in the LSV and WCD, the total integrated charge of each detector is used.

Additional information on the data acquisition, event reconstruction and detector calibrations can be found in [4, 18].

4. Data analysis and WIMP search

A dark matter search has been performed with data collected with atmospheric argon (AAr) target. Even with the reduced levels of ^{39}Ar in underground argon, if its activity is near the measured upper limit [19], ^{39}Ar β decay will still be the dominant background in DS-50. This initial AAr data set contains a sample of ^{39}Ar equal to that expected in a campaign of 23 years using UAr at the upper limit of ^{39}Ar activity. This allows a direct measurement of the ^{39}Ar background and an estimate of electron recoil background expected in DS-50 after all analysis cuts.

The initial dark matter search consists of the data set acquired between November 2013 and May, 2014. We excluded from the data set any runs where one of more of the detectors where not running and where the DAQ, still in a developmental phase, showed signs of instability. We applied a set of data quality cuts, both for the LAr TPC and the vetoes, to exclude backgrounds and misconstructed events. We accepted only events with all 38 TPC PMTs alive and with a baseline properly recognized in the channel representing the digital sum of all PMTs. We exclude pileup events selecting only events with a delayed physical start of at least 1.35 μs with respect to the physical start time of the previous event. Additionally, we reject the first event following a period of DAQ inaction of 1 second or more, indicating a stall of the DAQ.

We performed a non-blind physics analysis on the 53.4 days of WIMP search data. We discard LAr TPC events correlated to LSV activity. This cut excludes the prompt fraction of neutron captures and thermalization. The veto neutron cut is described in detail in [4].

Events containing exactly two pulses, S1 and S2, representative of expected elastic scattering on WIMPs are selected for further analysis. Also events with a S3 pulse, resulting from electrons released from the cathode when struck by the bright S2 UV light, are accepted for the WIMP search. Additionally, we require that the start time of the first reconstructed pulse is in the expected trigger position in the TPC DAQ window, and that the S1 does not saturate any of the PMTs. We require events whose S2 has f_{90} lower than 0.2, to remove fake S2 signals caused by re-triggering on a S1 signal, and a S2 pulse charge greater than 30 PE. The acceptance of the latter for nuclear recoils has been determined through a study of the SCENE2 data and it is compatible with unity [20].

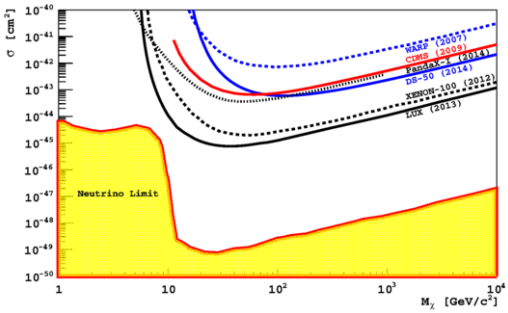

Figure 3: Spin-independent WIMP-nucleon cross section 90% C.L. exclusion plot for the DS-50 atmospheric argon campaign (Solid Blue Curve) compared with results from other WIMP direct detection experiments. Also shown is an approximate band (Yellow) where coherent scattering of solar [28, 29, 30], atmospheric, and diffuse supernova neutrinos begins to limit the sensitivity of direct detection experiments to WIMPs in absence of directional sensitivity. This picture has been taken from the DS-50 paper [4].

A fiducial cut in z was placed between 36.3 mm below the grid and above the cathode. The fiducial cut is defined by applying a cut on the drift time, requiring a drift time between 40.0 μs and 334.5 μs. The fiducial mass defined by this cut is (39.6 ± 0.6) kg.

We finally select events whose S1 falls in the selected WIMP search box, between 80 PE and 460 PE, corresponding to 38 keV and 206 keV respectively.

The accurate description of all cuts, their order of application, their effect on livetime, acceptance and fiducial volume, and their systematics and statistical uncertainties can be found on the analysis paper [4].

The total exposure (fiducial volume × livetime × acceptance) remaining after all cuts prior to the WIMP search box is (1423 ± 67) kg d. The distribution of the remaining events in the scatter plot of f_{90} vs. S1 after all quality and physics cuts is shown in Fig. 2. There are (15×10^6) events in this plot, dominated by ^{39}Ar decays.

This distribution of the remaining events in the scatter plot S1 vs f_{90} was studied by dividing the events into 5 PE-wide slices in S1, and fitting the resulting distributions with an approximate, analytical statistical model of f_{90} introduced in Ref. [21] and used in Ref. [22] to characterise the f_{90} distribution in LAr of a large statistics (1.6×10^7) sample of γ-ray scatters. The model

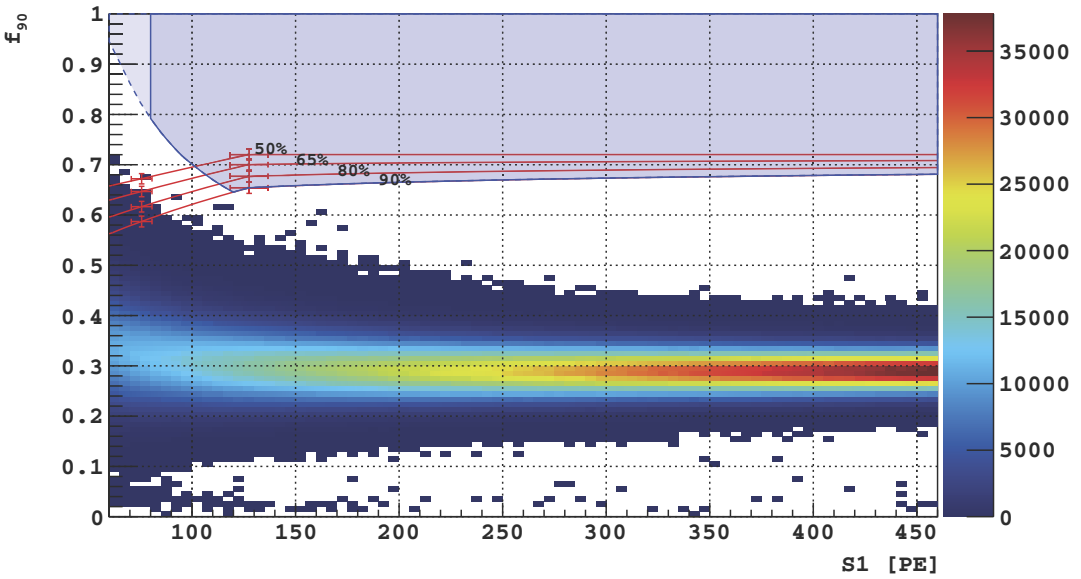

Figure 2: Distribution of the events in the scatter plot of S1 vs. f_{90} after all quality and physics cuts. Shaded Blue: dark matter search box in the f_{90} vs. S1 plane. Percentages label the f_{90} acceptance contours for nuclear recoils drawn connecting points (shown with error bars) determined from the corresponding SCENE measurements [20]. This picture has been taken from the DS-50 paper [4].

generally provides a good match to the tails of the experimental f_{90} distributions above 120 PE, while below this value the model slightly overestimates the tails.

Nuclear recoil acceptance curves in the f_{90} vs. S1 plane were derived from SCENE data and translated to DS-50. f_{90} median values from SCENE, linearly interpolated and assumed to be constant above the highest SCENE NR energy, are translated from the SCENE nuclear recoil energies to DS-50 S1 values. This gives the 50% contour for DS-50. The other contours and associated errors depend also on the width of the DS-50 f_{90} distributions at each S1, which is established using the same analytical model in use to described the f_{90} spread for ^{39}Ar events described above. These curves are shown in Fig. 2.

We observe 4 events passing all TPC cuts and with nuclear-recoil-like f_{90}, but with energy depositions in the LSV above our veto cut threshold. In coincidence with one of these 4 neutron candidates, we recorded signals near saturation in both the LSV and the WCD, and therefore we classify that event as a cosmogenic neutron [23], leaving 3 radiogenic neutron candidates. This number is in agreement with the neutron-induced events passing all TPC cuts expected from radiogenic neutrons from the PMTs based on Monte Carlo studies.

To derive a dark matter limit from Fig. 2, we assume the standard isothermal-WIMP-halo model [24, 25] with v_{esc} = 544 km/s [26], v_0 =220 km/s [26], v_{Earth} = 232 [27], ρ_{DM} = 0.3 GeV/cm^3 [25]. Given the null result shown in Fig. 2, we derive a 90% C.L. exclusion curve corresponding to the observation of 2.3 events for spin-independent interactions, and we compare it in Fig. 3 with limits from recent experiments.

5. Conclusions and outlook

The DarkSide-50 direct dark matter detection system has completed his first physics data taking at LNGS.

The dark matter box in Fig. 2 covers the range of energies from 8.6 to 65.6 keV for ^{39}Ar, and a total of 15×10^6 ^{39}Ar β-decays were recorded over that energy range. Event selection based on the TPC cuts is shown to completely suppress ^{39}Ar background events in the present (1423 ± 67) kg d exposure.

This exposure contains at least as many ^{39}Ar decays as 215000 kg d of running with underground argon, proving that DS-50 could run for two decades with underground argon and be free of ^{39}Ar background.

Although the liquid scintillator veto was compromised by a high ^{14}C content during this exposure, it was able to tag and remove the handful of neutron events expected. In the underground argon run, we will be operating with a neutron veto that will be able to sustain

lower thresholds, predicted to give considerably higher neutron detection efficiency.

A WIMP search with the present data-set gives a limit as low as 6.1×10^{-44} cm^2, the best result achieved to date with an argon target. This is the first walk on the DarkSide.

The DarkSide program is supported in the USA by the NSF and the DOE and in Italy by INFN. We gratefully acknowledge the hospitality of Laboratori Nazionali del Gran Sasso (LNGS). The author acknowledges the support of University of Houston.

References

[1] K.A. Olive et al. (Particle Data Group), Chin. Phys. C, 38, 090001 (2014)
[2] P. Benetti et al. (WARP Collaboration), Astopar. Phys. 28, 495 (2008)
[3] M.G. Boulay and A. Hime, Astropart. Phys. 25:179 (2006)
[4] T. Alexander et al. (DarkSide Collaboration), arXiv:1410.0653 [astro-ph.CO]
[5] G. Alimonti et al. (Borexino Collaboration), Astropart. Phys. 8, 141 (1998) doi:10.1016/S0927-6505(97)00050-9.
[6] G. Alimonti et al. (Borexino Collaboration), Nucl. Instr. Meth. A **406**, 411 (1998) doi:10.1016/S0168-9002(98)00018-7.
[7] G. Bellini et al.(Borexino Collaboration), JINST 6 P05005 (2011) doi:10.1088/1748-0221/6/05/P05005
[8] G. Bellini et al. (Borexino Collaboration), JCAP **05**, 015 (2012) doi:10.1088/1475-7516/2012/05/015
[9] G. Alimonti et al. (Borexino Collaboration), Nucl. Instr. Meth. A **600**, 568 (2009) doi:10.1016/j.nima.2008.11.076.
[10] G. Alimonti et al. (Borexino Collaboration), Nucl. Instr. Meth. A **609**, 58–78 (2009) doi:10.1016/j.nima.2009.07.028.
[11] G. Bellini et al. (Borexino Collaboration), Phys. Rev. Lett. **107**, 141301 (2011) doi:10.1103/PhysRevLett.107.141302.
[12] G. Bellini et al. (Borexino Collaboration), Phys. Rev. D **89**, 112007 (2014) doi:10.1103/PhysRevD.89.112007.
[13] A. Wright, P. Mosteiro, and F. Calaprice, Nucl. Instr. Meth. A **644**, 18 (2011) doi:10.1016/j.nima.2011.04.009.
[14] T. Alexander et al. (DarkSide Collaboration), Astropart. Phys. **49**, 44 (2013) doi:10.1016/j.astropartphys.2013.08.004.
[15] Stefano Davini, Nucl. Instrum. Meth. **A** 742 183-186 (2014), doi:10.1016/j.nima.2013.10.066
[16] T. Alexander et al. (DarkSide Collaboration), JINST 8 C11021 (2013) doi:10.1088/1748-0221/8/11/C11021
[17] C. Aalseth et Al., The DarkSide multi-ton detector for the direct dark matter search, Advances in High Energy Physics, Accepted June 2014 (http://www.hindawi.com/journals/ahep/raa/541362)
[18] DS-50 Electronics paper in preparation
[19] J. Xu et al., arxiv1204.6011.
[20] T. Alexander et al. (SCENE Collaboration), arxiv:1406.4825.
[21] W. H. Lippincott, K. J. Coakley, D. Gastler, A. Hime, E. Kearns, D. N. McKinsey, J. A. Nikkel, and L. C. Stonehill, Phys. Rev. C **78**, 035801 (2008)
[22] M. G. Boulay et al. (DEAP Collaboration), arxiv:0904.2930.
[23] G. Bellini et al. (Borexino Collaboration), JCAP **08**, 049 (2013), doi:10.1088/1475-7516/2013/08/049
[24] J. D. Lewin and P. Smith, Astropart. Phys. **6**, 87 (1996)
[25] C. Savage, K. Freese, and P. Gondolo, Phys. Rev. D **74**, 043531 (2006)
[26] M. C. Smith et al., Mon. Not. Roy. Astron. Soc. **379**, 755 (2007)
[27] C. Savage, G. Gelmini, P. Gondolo, and K. Freese, JCAP **0904**, 010 (2009)
[28] G. Bellini et al. (Borexino Collaboration), Nature 512 (2014) 7515, 383-386 doi:10.1038/nature13702
[29] G. Bellini et al. (Borexino Collaboration), Phys. Rev. Lett. 108 (2012) 051302 doi:10.1103/PhysRevLett.108.051302
[30] G. Bellini et al. (Borexino Collaboration), Phys. Rev. D 82 (2010) 033006 doi:10.1103/PhysRevD.82.033006